ON THE RELATIONSHIP BETWEEN PMSE STRENGTH AND PARTICLE PRECIPITATION

Tarjei Antonsen and Ove Havnes

University of Tromsø, PO.Box 6050 Langnes, 9037 Tromsø, Norway

ABSTRACT

We have studied the relationship between particle precipitation and PMSE strength on days where we observe PMSE layers both with the EISCAT VHF and UHF radars. The UHF observations of the ionization and its variation, above the PMSE layer, is used as a measure of precipitation. Variations of the precipitation is compared with variations of the PMSE strengths observed with both radars. Although many cases apparently show a clear connection between precipitation and PMSE, where an increased precipitation leads to a strengthening of the PMSE, our findings confirm that there is no general and simple proportionality between the two. For the weakest PMSE there appears to be no correlation between precipitation and PMSE strength. For PMSEs around average strength of our observations there appears to be a weak positive correlation, which can be predicted by a time-dependent dust cloud charge model. On some occasions an increased precipitation can, apparently, initially lead to an increase of PMSE strength which at some point starts to decline even if the precipitation continue to increase. This feature can also be seen in the results from the statistical analysis, however the number of occurrences is too low to conclude with significance and the time-dependent charge model described here does not reproduce such features. We have studied to what degree models for the PMSE scattering can explain the various cases of reaction of PMSE to changes in precipitation.

1. INTRODUCTION

Since the first observations were made of strong coherent radar echoes from the polar mesosphere in the late 1970's and early 80's [5, 7], this phenomenon; so called Polar Mesospheric Summer Echoes (PMSE) (see Rapp and Lübken [21] for a review); have been central in the study of the upper mesosphere. The PMSE originates from radar scattering at coherent length scales from icy dust clouds residing around the polar summer mesopause, which is the coldest place on earth with temperatures reaching as low as 110 K [17].

Several studies have investigated the diurnal and annual variations of PMSE with precipitation measures such as cosmic noise absorption (CNA), the K-index and the F10.7 flux [16, 3, 4, 18, 23, 1, 24]. In general, the studies find weak positive correlation factors between CNA and PMSE strength. For the K-index and F10.7 flux, the studies disagree about the significance of the effect of precipitation [23, 4]. In review, these studies provide evidence of a causal relationship between electron density and PMSE strength, however it is clear that the relationship is not simple.

In the present paper we present the first results from a statistical analysis of the response of VHF and UHF PMSE to precipitation. We exclusively study the correlation on short timescales, i.e. response times from zero seconds to several tens of seconds; which is comparable to PMSE charging times. The data used is VHF and UHF radar data acquired at EISCAT Ramfjordmoen (69.58° N 19.21° E) during the summer campaign of 2004 (see [19]). This is due to the high quality of the data and high occurrence rate of PMSE, with echoes present 95% of the time on the VHF radar and 11% of the time on the UHF radar. Details about the radar data and its analysis is presented in section 2. The results from the statistical analysis are presented in section 4 and furthermore discussed in section 5 in context of the time-dependent dust cloud charge model (see e.g. Havnes [10]) described in section 3. On the basis of this discussion, we conclude that there is a weak positive correlation between PMSE strength and rapid changes in electron density for (moderately) strong echoes. This feature can be explained by the presented model as a function of the plasma parameters represented by the P-value (see e.g. Havnes [10]).

2. RADAR DATA AND CORRELATION PROCEDURE

The experimental data analyzed here was collected at 0800-1000 UT on the 7th, 13th and 14th of July 2004, following the discovery of the PMSE overshoot effect one year earlier [10, 12]. All of the time series contain both VHF (224 MHz) and UHF (931 MHz) PMSE, which were sometimes simultaneous. The data shows PMSE during a wide range of ionospheric and mesospheric ambient conditions. Figure 1 shows one hour of VHF data (top panel) and UHF data (bottom panel) obtained on the

Proc. '22nd ESA Symposium on European Rocket and Balloon Programmes and Related Research',
Tromsø, Norway, 7–12 June 2015 (ESA SP-730, September 2015)

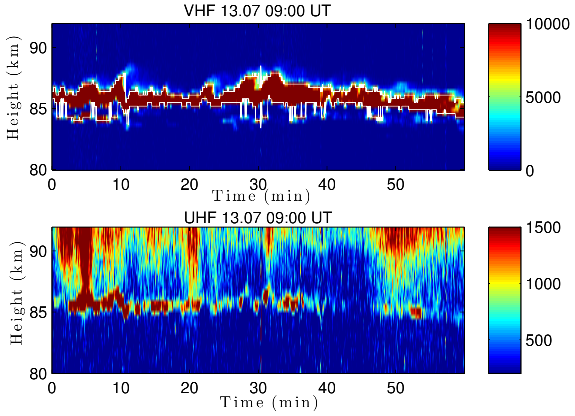

Figure 1. Height-time plot of arbitrary PMSE intensity for VHF (top) and UHF (bottom) starting at the 13th of July 0900 UT.

13th of July between 0900 and 1000 UT. This example displays the strongest precipitation values and PMSE occurrence rate encountered during the 2004 campaign. A conspicuous feature of this time series is the occasional very strong precipitation reaching down in to the mesosphere, as observed in the UHF data. This precipitation often seems to coincide in time with the strongest UHF PMSE seen around 86 km altitude. For other time series, especially during weak to moderate PMSE, such coincidences are not as consistent.

To investigate the relationship between precipitation and PMSE, a measure of these two must be defined. We define a one-dimensional time-dependent measurement of the PMSE strength by simply taking the maximum value inside the layer (defined as inside the white borders in fig. 1). Other measures such as the minimum, median and mean PMSE strength have been tested, with very similar results. The precipitation measure is defined by first fitting an exponential function to the UHF data between 90 and 100 km (30 height bins) and extrapolate the curve down to the altitude of the maximum PMSE value. Furthermore we calculate the correlation between the two measures by dividing the precipitation into chains where the time development is monotonic and calculating the correlation coefficient with Spearman rank analysis. In this way we can robustly extract a strict relationship between precipitation and PMSE strength if there is one. As discussed below, we also perform the calculation for a range of time lag values. Figure 2 shows a schematic of the procedure.

3. TIME-DEPENDENT DUST CLOUD CHARGE MODEL

One of the main reasons for doing a correlation analysis like the present, is to resolve issues regarding the physical mechanisms of PMSE. We therefore here employ a time-dependent simultaneous cloud v. grain charge model, in-

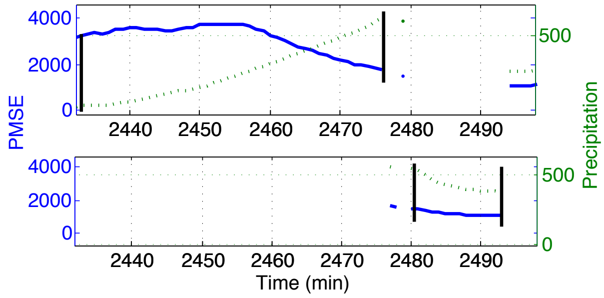

Figure 2. Correlation procedure where monotonic gradients of precipitation (green dotted line), is correlated with PMSE strength (solid line).

troduced in Havnes et al. [11]. Following the approach of Havnes [10] we generalize to allow for unequal electron and ion temperatures.

Firstly, for electrons (e) and ions (i) in the background plasma (with $n_{e0} = n_{i0} = n_0$) the electric forces are assumed to balance the pressure gradients so densities become Boltzmann distributed:

$$n_{e,i} = n_0 \exp\left(-\frac{Z_{e,i}eV}{k_B T_{e,i}}\right) \tag{1}$$

where $Z_{e,i}$ is the charge number, V is the plasma potential, k_B is the Boltzmann constant and $T_{e,i}$ is the ambient electron or ion temperature.

To calculate the reaction time (or charging time) of the PMSE cloud, we calculate the electron current to a grain in equilibrium. For grains of sizes found in PMSE ($\gtrsim 20$ nm) we can use average charge. We neglect dust polarizing effects such that the electron current to a grain becomes [6]:

$$I_e = \pi r_d^2 s_e c_e n_e \exp\left(\frac{eU}{k_B T_e}\right) \tag{2}$$

where r_d is the dust radius, $c_e = (8kT_{e,i}/\pi m_{e,i})^{1/2}$ is the mean electron thermal speed and $U = Z_d e/4\pi\epsilon_0 r_d$ is the dust grain surface potential. The electrons are assumed to have a sticking probability of $s_e = 1/2$.

Havnes et al. [11] has argued that for PMSE relevant plasma parameters, the plasma approximation can replace Poisson's equation. It can accordingly be shown that the dust surface potential and cloud potential can simultaneously be described by:

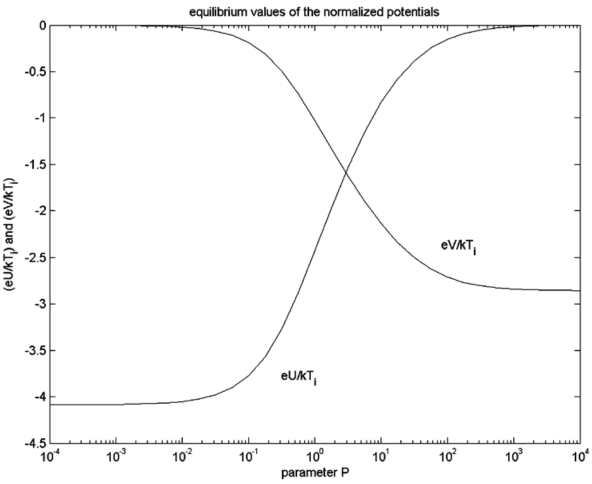

Figure 3. Figure from Havnes [10] of the variation of normalized cloud and dust grain potentials with the P-value. Here, the plasma is thermailzed with $T_e = T_i$.

$$\frac{\mathrm{d}\widehat{\mathrm{U}}}{\mathrm{d}t} = \frac{e^2 r_d n_0}{4\epsilon_0 k_B T_i} \times ... \left[-c_e \exp\left(\left(\widehat{U}+\widehat{V}\right)\frac{T_i}{T_e}\right) + c_i \exp\left(-\widehat{V}\right)\left(1-\widehat{U}\right)\right] \tag{3}$$

$$\exp\left(\frac{T_i}{T_e}\widehat{V}\right) - \exp\left(-\widehat{V}\right) - P\widehat{U} = 0 \tag{4}$$

where $\widehat{U} = eU/k_B T_i$ and $\widehat{V} = eV/k_B T_i$ are the normalized dust surface and cloud potentials and e the elementary charge. The parameter P is [11, 10]:

$$P = \frac{4\pi\epsilon_0 r_d n_d k_B T_i}{e^2 n_0}. \tag{5}$$

This parameter is an ordering parameter for the grain v. cloud charge problem, and at the short timescales we investigate here, the most important proportionality is the one of n_e^{-1}. In equilibrium, as pointed out by Havnes et al. [11], the normalized potentials are solely functions of the P-value. Havnes et al. [14] developed analytical approximations of the normalized potentials as function of the P-value. For very low values of P, the approximation becomes linear in $\widehat{V}$. Figure 3 gives an example of the development of the normalized potentials in equilibrium with P. It can be shown by insertion into eq. (6) that for low P-values, the change in the $\widehat{V}$-potential (developed to first degree in P) is equal to the change in P, so that a change in the external electron density does not affect the PMSE strength.

Ginzburg [9] showed that the volume reflection of coherent echoes is proportional to $(\Delta n_e)^2$. Havnes et al. [13] and Biebricher et al. [2] have adapted this to the time dependent dust charge model, such that the relative PMSE backscatter becomes:

$$R \propto \left[\frac{n_{e,C}(t) - n_{e,0}(t)}{n_{e,C}(0) - n_{e,0}(0)}\right]^2 = \left[\frac{n_{e,p}\exp(\widehat{V}_p) - n_{e,p}}{n_{e,0}\exp(\widehat{V}_0) - n_{e,0}}\right]^2 \tag{6}$$

where $n_{e,C}(t)$ is the electron density in the center of the PMSE scattering structure at time t, $n_{e,0}(t)$ is the background density and $n_{e,p}$ is the electron density moderated by precipitation.

4. RESULTS

The diurnal variation of the ionospheric D-layer conditions was significant between the different data sets examined here. This means that the results from the analysis should represent a more general picture of the PMSE-precipitation relationship as opposed to a case study.

Results from the statistical analysis of the relationship between precipitation and VHF PMSE is shown in figure 4. The scatter plot consists of 747 correlation coefficients for monotonic precipitation gradients for the no lag case. We see no clear bunching, however, the distribution in the lower panel shows a tendency to an increase in the number of coefficients around ~ 0.5. The overall shape of the distribution indicate that there is a weak positive correlation on a background of no correlation. Figure 5 investigates this relationship further by presenting the distribution of correlation coefficients as a function of PMSE strength. Here, the uniformly distributed values below a strength of $22 \cdot 10^3$ arbitrary units, which is around the average measured PMSE strength, have been removed. For the sake of clarity, we present there the correlation for 8 seconds of lag for reasons explained below. For moderately strong PMSE (first panel), the flat distribution indicate that the peak around 0.5 show that there is some preference for a positive correlation. For the second panel the positive correlation is less general, and contain a few more negative coefficients, and coefficients around zero. For the strongest PMSE in the third panel the situation is more unclear but may indicate that there is a tendency for a negative correlation. The low number of these occurrences prohibits conclusion with significance. We do not find that an anti-correlation can be explained by the simple cloud charge model presented here.

We do not present here the results from the UHF analysis. The number of coefficients is too low too conclude with significance, however, with the limited data available the distribution becomes nearly Gaussian, proposing that that the effect of precipitation is not as pronounced in UHF PMSE as in its VHF counterpart. This may be due to that the UHF PMSE have a tendency to occur only in the stronger parts of the VHF PMSE layers [19].

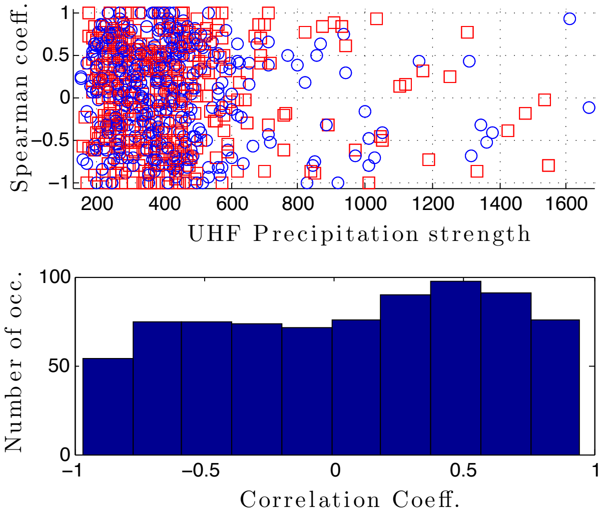

Figure 4. Scatter plot (top) and distribution (bottom) of Spearman (no lag) correlation coefficients for VHF echoes versus precipitation compared to precipitation strength. The red squares denote negative gradients and the blue circles represent positive gradients in precipitation.

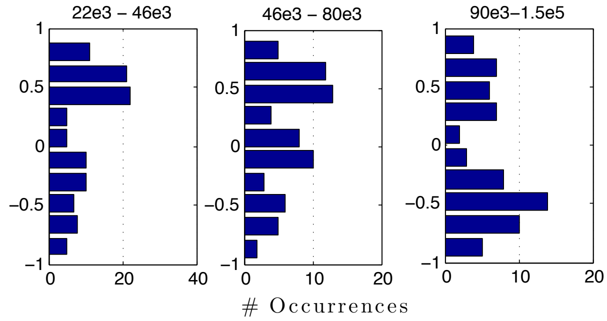

Figure 5. Distribution of correlation coefficients at a time lag of eight seconds for different bins of PMSE strength. The bin range is indicated above the panels, and is set such that the number of values in each bin are comparable.

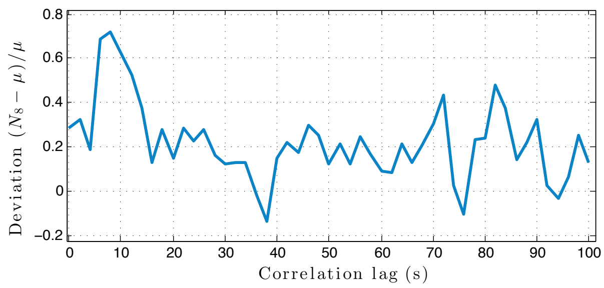

Figure 6. Relative deviation between bin 8 (coefficients ~ 0.5) and the mean value of the rest of the bins, as a function of lag.

5. DISCUSSION AND CONCLUDING REMARKS

Our findings regarding the PMSE v. precipitation relationship presented in this work will benefit from a clear connection to a theory describing the reaction of the PMSE layer to electron precipitation. For this purpose, we investigate the validity of our findings in the framework of the time-dependent cloud charge model presented above.

The average length of chains of precipitation which increases monotonically is on the order of several tens of seconds. It may then be expected that a relatively short lag, of say a few seconds due to cloud charging inertia, would yield very similar result as the no lag analysis carried out here. This follows from the nature of the Spearman rank analysis; 'outliers' and short timescale irregularities are not strongly emphasized. If the charging time was large compared to the average chain length, problems may arise. When doing the same correlation analysis for several lag values, bin number eight in fig. 4 is with few exceptions the largest. In figure 6 we show the development of the size of this bin as a function of lag time. At around 10 seconds lag, the bin has its relative largest value ($\sim 70\%$ larger than the mean at $t = 8s$). For illustrative purposes, we chose the eight second lag in figure 5 to best show the strength of the PMSE-precipitation relationship as a function of echo strength. A possible explanation of the enhanced correlation at these time lags may be that the characteristic timescale of charging mechanisms to introduce sharp electron density gradients (and thereof in PMSE strength) is around 10 seconds.

In figure 7 we show calculations of the charging time of dust grains of different sizes in equilibrium as a function of electron density (range of n_e based on Friedrich and Rapp [8]). For electron density values between 10^9 and 10^{10} m^{-3}, as calculated for our data by Næsheim et al. [19], charging times range from 1 to 100 second depending on the dust radius. For larger particles, a charging time of around 10 seconds is reasonable, indicating that the correlation lag analysis has a certain validity.

We also need to compare our findings of no or very weak correlation at low PMSE strength and a weak correlation for moderately strong PMSE with the introduced cloud charge model. When utilizing the polynomial approximation of Havnes et al. [14] at small P-values ($\widehat{V}$ becomes approximately linear in P) we calculate a relative PMSE backscatter with eq (6) of $R \approx 1$ for all reasonable changes in n_e; significant strengthening of precipitation does not alter the PMSE strength. Correspondingly, for higher values of P ($\widehat{V}$ is a function of P^2), a change in P from 0.2 to 0.1 which is a doubling i n_e induces a relative backscatter of $R = 1.8$; precipitation strengthens the PMSE backscatter. Figure 8 shows the calculated relative PMSE backscatter by eq. (6) for a range of P-values and electron density enhancements. From eq. (5) we find that PMSE conditions leading to values of P comparable to 1 will be hard to find. In addition to this it is clear that there cannot be a linear relationship between P and the strength of PMSE scattering. Havnes et al. [15] finds

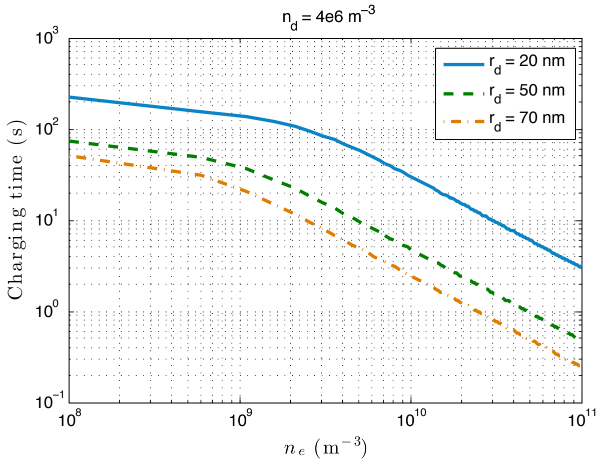

Figure 7. The time of dust grains in equilibrium of three different sizes to acquire 0.3 additional negative charges as a function of electron density. Electrons and ions are assumed here to be thermalized.

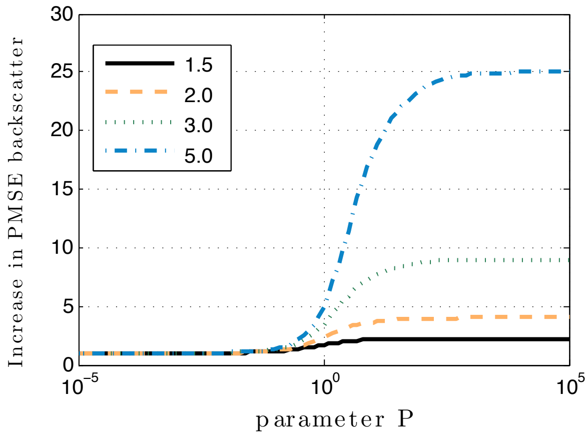

Figure 8. Variation of PMSE backscatter intensity as a function of P-value for different temporary enhancements of the background electron density (enhancement factors in legend). It seems clear that P-values of the order of one or larger are very unlikely for PMSE conditions.

a linear relationship for P less than ca 0.1, and a small change in PMSE strength up to $P \approx 0.6$ followed by a decrease above this.

As discussed above, for small P-values, the PMSE strength remains unchanged even for large intensifications of ambient electron density. For $P \sim 1$, we observe that $R \sim \Delta n_e$. If Havnes et al. [15] is correct this may imply that for the weak PMSE there is a mixture of cases with low and with high P, leading to a mixture of cases with no correlation with precipitation and (few) cases with linear correlation. This might explain the observed results for weak and moderately strong PMSE. Our results are obtained with a relatively simple dust model. This model will in future works be extended to include effects which are important in PMSE clouds with high dust density such as the electron bite outs [20].

In general, from out findings, it can be stated that VHF PMSE has a tendency to a weak positive correlation with precipitation only when the strength of the echoes is comparable to the mean value of PMSE corresponding to $\approx 2.5 \cdot 10^4$ arbitrary units cf. fig. 5.

We have found that there is no strong or clear correlation between PMSE strength and precipitation. For echo strengths above average, a tendency to positive correlation have been found and for the strongest observed echoes, anti-correlation may be present. This latter feature cannot be reproduced with the simple cloud charge model described here. The P-value from eq. (5) has been shown to act as a reasonable ordering parameter of the effect of precipitation on PMSE strength in the regime. Rapp and Lübken [22] also presented a proxy for the variation of PMSE strength, with $P_R = |Z_d| n_d r_d^2$, however it is difficult to apply to the case of precipitation due to the lack of n_e in the expression. Nevertheless, more PMSE data from VHF and UHF simultaneously is needed to get a complete understanding of both general and more rare precipitation-PMSE strength relationships.

REFERENCES

[1] Barabash, V., Kirkwood, S., and Chilson, P. B. Are variations in PMSE intensity affected by energetic particle precipitation? *Annales Geophysicae*, 20(4): 539–545, 2002. doi: 10.5194/angeo-20-539-2002.

[2] Biebricher, A., Havnes, O., Hartquist, T.W., and LaHoz, C. On the influence of plasma absorption by dust on the PMSE overshoot effect. *Advances in Space Research*, 38(11): 2541 – 2550, 2006. ISSN 0273-1177. doi: http://dx.doi.org/10.1016/j.asr.2005.02.061.

[3] Bremer, J., Hoffmann, P., and Hansen, T. L. Geomagnetic control of polar mesosphere summer echoes. *Annales Geophysicae*, 18(2):202–208, 2000.

[4] Bremer, J., Hansen, T.L., Hoffmann, P., and Latteck, R. Dependence of polar mesosphere summer echoes on solar and geomagnetic activity. *Advances in Space Research*, 28(7):1071 – 1076, 2001. ISSN 0273-1177. doi: http://dx.doi.org/10.1016/S0273-1177(01)80039-9.

[5] Czechowsky, P., Rüster, R., and Schmidt, G. Variations of mesospheric structures in different seasons. *Geophysical Research Letters*, 6(6):459–462, 1979. ISSN 1944-8007. doi: 10.1029/GL006i006p00459.

[6] Draine, B. T. and Sutin, B. Collisional charging of interstellar grains. *ApJ*, 320:803–817, 1987. doi: 10.1086/165596.

[7] Ecklund, W. L. and Balsley, B. B. Long-term observations of the arctic mesosphere with the MST radar at poker flat, alaska. *Journal of Geophysical Research: Space Physics*, 86(A9):7775–7780, 1981. ISSN 2156-2202. doi: 10.1029/JA086iA09p07775.

[8] Friedrich, M. and Rapp, M. News from the lower ionosphere: A review of recent developments. *Surveys in Geophysics*, 30(6):525–559, 2009. ISSN 0169-3298. doi: 10.1007/s10712-009-9074-2.

[9] Ginzburg, V.L. *The propagation of electromagnetic waves in plasmas*. International series of monographs on electromagnetic waves. Pergamon Press, 1970.

[10] Havnes, O. Polar mesospheric summer echoes (pmse) overshoot effect due to cycling of artificial electron heating. *Journal of Geophysical Research: Space Physics*, 109(A2), 2004. ISSN 2156-2202. doi: 10.1029/2003JA010159.

[11] Havnes, O., Morfill, G. E., and Goertz, C. K. Plasma potential and grain charges in a dust cloud embedded in a plasma. *Journal of Geophysical Research: Space Physics*, 89(A12): 10999–11003, 1984. ISSN 2156-2202. doi: 10.1029/JA089iA12p10999.

[12] Havnes, O., La Hoz, C., Næsheim, L. I., and Rietveld, M. T. First observations of the PMSE overshoot effect and its use for investigating the conditions in the summer mesosphere. *Geophysical Research Letters*, 30(23):16–1–15–4, 2003. ISSN 1944-8007. doi: 10.1029/2003GL018429.

[13] Havnes, O, Hoz, C La, Biebricher, A, Kassa, M, Meseret, T, Næsheim, I, and Zivkovic, T. Investigation of the mesospheric pmse conditions by use of the new overshoot effect. *Physica Scripta*, 2004(T107):70–78, 2004. doi: 10.1238/Physica.Topical.107a00070.

[14] Havnes, Ove, Aanesen, Torsten K., and Melandsø, Frank. On dust charges and plasma potentials in a dusty plasma with dust size distribution. *Journal of Geophysical Research: Space Physics*, 95 (A5):6581–6585, 1990. ISSN 2156-2202. doi: 10.1029/JA095iA05p06581.

[15] Havnes, Ove, Aslaksen, Torsten, and Brattli, Alvin. Charged dust in the earth's middle atmosphere. *Physica Scripta*, 2001(T89):133, 2001. doi: 10.1238/Physica.Topical.089a00133.

[16] Klostermeyer, J. On the diurnal variation of polar mesosphere summer echoes. *Geophysical Research Letters*, 26(21):3301–3304, 1999. ISSN 1944-8007. doi: 10.1029/1999GL003629.

[17] Lübken, F.-J., Lautenbach, J., Hffner, J., Rapp, M., and Zecha, M. First continuous temperature measurements within polar mesosphere summer echoes. *JASTP*, 71(3–4):453–463, 2009. ISSN 1364-6826. doi: http://dx.doi.org/10.1016/j.jastp.2008.06.001.

[18] Morris, R. J., Terkildsen, M. B., Holdsworth, D. A., and Hyde, M. R. Is there a causal relationship between cosmic noise absorption and PMSE? *GRL*, 32:L24809, 2005. doi: 10.1029/2005GL024568.

[19] Næsheim, LI, Havnes, O, and La Hoz, C. A comparison of polar mesosphere summer echo at VHF (224 mhz) and uhf (930 mhz) and the effects of artificial electron heating. *Journal of Geophysical Research: Atmospheres (1984–2012)*, 113(D8205), 2008. doi: 1029/2007JD009245.

[20] Pedersen, A., Troim, J., and Kane, J.A. Rocket measurements showing removal of electrons above the mesopause in summer at high latitude. *Planetary and Space Science*, 18(6):945 – 947, 1969. ISSN 0032-0633. doi: http://dx.doi.org/10.1016/0032-0633(70)90092-9.

[21] Rapp, M. and Lübken, F.-J. Polar mesosphere summer echoes (PMSE): Review of observations and current understanding. *Atmospheric Chemistry and Physics*, 4(11/12):2601–2633, 2004. doi: 10.5194/acp-4-2601-2004.

[22] Rapp, Markus and Lübken, Franz-Josef. On the nature of pmse: Electron diffusion in the vicinity of charged particles revisited. *Journal of Geophysical Research: Atmospheres*, 108(D8):4–1–4–13, 2003. ISSN 2156-2202. doi: 10.1029/2002JD002857.

[23] Smirnova, M., Belova, E., and Kirkwood, S. Polar mesosphere summer echo strength in relation to solar variability and geomagnetic activity during 1997–2009. *Annales Geophysicae*, 29(3):563–572, 2011. doi: 10.5194/angeo-29-563-2011.

[24] Zeller, O. and Bremer, J. The influence of geomagnetic activity on mesospheric summer echoes in middle and polar latitudes. *Annales Geophysicae*, 27(2):831–837, 2009. doi: 10.5194/angeo-27-831-2009.